www.amlett.org, www.amlett.com, DOI: 10.5185/amlett.2013.icnano.146
"ICNANO 2011" Special Issue Published online by the VBRI press in 2013

Gas sensing and dielectric studies on cobalt doped hydroxyapatite thick films

Megha P. Mahabole[1], Ravindra U. Mene[1,2] and Rajendra S. Khairnar[1*]

[1]*School of Physical Sciences, S.R.T.M. University, Nanded 431606, India*
[2]*School of Engineering, Matoshri Group of Institutions, Nanded 431606 (MS), India*

*Corresponding author: E-mail: rskhairnarsps@gmail.com

ABSTRACT

This present paper deals with the investigation on effective utilization of cobalt doped hydroxyapatite (Co-HAp) thick films for improvement in gas sensing and dielectric properties. Chemical precipitation route is used for synthesis of nanocrystalline hydroxyapatite (HAp) bioceramic and ion exchange process is carried out for the partial substitution of cobalt ions in HAp matrix. Hydroxyapatite thick films, prepared using screen printing technique, are used as samples for gas sensing and dielectric measurements. The structural identification of HAp thick films is carried out using X-ray diffraction and the presence of functional groups in pure and doped HAp is confirmed by means FTIR spectroscopy. The surface morphology of these films is visualized by means of SEM and AFM analysis. Detailed study on CO_2 gas sensing performance of pure and Co-HAp thick films is carried out wherein operating temperature, response/recovery times and gas uptake capacity are determined. It is remarkable to note that Co-HAp film with 0.01M cobalt concentration shows maximum sensitivity to CO_2 gas at relatively lower operating temperature of 135^{o}C in comparison with pure HAp as well as other concentrations of cobalt doped HAp films. The frequency dependent variation of dielectric constant (K) and dielectric loss (tan δ) of HAp thick films are also studied in the range of 10 Hz-1MHz at room temperature. The result shows that increase of cobalt concentration in HAp matrix leads to increase in dielectric constant. The study reveals clear influence of cobalt substitution on dielectric properties and gas sensing properties HAp matrix.

Keywords: Hydroxyapatite; screen printing process; thick films; gas Sensor; dielectric study; XRD; AFM.

Megha P. Mahabole has received her Ph.D. in 2005 from SRTM University, Nanded, India. Currently she is an Associate Professor at School of Physical Sciences, SRTM University, Nanded. She has more than 12 years of experience in teaching and research field. Her research areas are synthesis and characterization of hydroxyapatite biomaterial, gas sensor, natural and synthetic zeolites.

Ravindra U Mene has received his post-graduate and Ph.D degrees in the year 2006 and 2012 from the School of Physical Sciences, SRTM University, Nanded. Presently he is working as a Assistnat professor in School of Engineering, Matoshri Pratisthans Group of Institution, Nanded. His current research interests are surface modified nano-ceramics and ion-exchanged nano-material used for gas sensing application.

Rajendra S. Khairnar had received Ph.D. degree in Field Electron Emission and Ion Microscopy from University of Pune, India in 1989. He was Scientist at Central Electronics Engineering Research Institute at Pilani, India during 1991-1996. He is working in the area of electron emitters, dispenser cathodes, Nano-materials, optical fiber sensors, gas sensors, Nano-biomaterial, mediated extremophiles and zeolites. Presently, he is Director of School of Physical Sciences at SRTM University, Nanded, India.

Introduction

Demand for chemical sensors is increasing in recent years because they play an important role in various areas like emission control, environmental protection, public safety, and human health **[1-2].** Therefore, there is a need of development of new sensors capable of detecting the target gases with high sensitivity and quick response. There are number of ways to upgrade the sensitivity of a known sensor by some magnitude. Adding dopant to a sensor matrix is one of the best known ways to enhance the sensor

characteristics **[3-4].** Bioceramic hydroxyapatite [HAp,$Ca_{10}(PO_4)_6(OH)_2$] is widely used for bone and tissue engineering because of its chemical similarity to natural bone and excellent biocompatibility **[5].** Moreover, it finds other prospective applications in various fields such as catalyst **[6],** ion exchanger **[7],** electrolyte for high temperature fuel cell **[8],** protein separation **[9],** and biosensors **[10].** Recently, it has received considerable attention as a chemical gas sensor due to its peculiar properties such as presence of large surface P-OH groups which interacts with the gas molecules to be sensed, highly porous structure and capability to exchange ions **[11-13].**

The hydroxyapatite crystal structure composed of variety of ions namely $(PO_4)^{3-}$, OH^-, and Ca^{2+} and possesses excellent ion exchange capacity. The Ca^{2+} ions in the crystal can very easily be replaced by various divalent metal cations like Sr^{2+}, Mg^{2+}, Cd^{2+}, Mn^{2+}, Pb^{2+}, Co^{2+}, Ba^{2+}, Ni^{2+} and Zn^{2+}. It is not only possible to exchange PO_4^{3-} groups with such anions as CO_3^{2-}, SO_3^{2-} but also to replace OH^- groups by F^- and Cl^- anions **[14-24].** Literature survey reveals that ion exchange capability of HAp is utilized for various applications. Stanic et al, have studied the use of Cu and Zn doped hydroxyapatite nano-material for antimicrobial activity **[25].** The efficient use of strontium doped hydroxyapatite nano-rods for drug loading and controlled release of ibuprofen (IBU) is reported by Zhang et al. **[26].** The work on Mn doped hydroxyapatite for in-vitro bioactivity study using human osteoblast cells is carried out by Paluszkiewicz et al. **[27].** Mabilleau et al. have reported effect of addition of cobalt, chromium and nickel metal ions in hydroxyapatite during in-vitro crystal growth process **[28].** Magnetic properties of cobalt-ferrite doped hydroxyapatite are also studied by Petchsang et al. **[29].** The metal ion sorption and exchange behavior of HAp is also used for the removal of heavy metal ions such as Pb, Zn, Cu, Cd, Co and Sb from waste water or soils **[30-35].** But the use of ion exchanged HAp in chemical sensor field remains untended. The study on gas sensing performance of pure and swift heavy ion irradiation (SHI) modified HAp, for CO and CO_2 gases, is carried out by our group wherein sensor performance is found to be improved upon SHI irradiation **[11-12].** However, detailed investigation on cobalt metal ion exchanged HAp for sensing target gas has not been reported so far.

Hence, the present paper reports the investigation on influence of the cobalt doping on dielectric and gas sensing properties of HAp matrix. Cobalt doped hydroxyapatite is characterized by XRD, FTIR, SEM and AFM. The studies on dielectric properties and gas sensing characteristics for CO_2 gas sensor are carried out.

Experimental

Material synthesis

Chemical precipitation route is used for the synthesis of nano-ceramic HAp. Calcium nitrates ($Ca(NO_3)_2.4H_2O$), and di-ammonium hydrogen phosphate ($(NH_4)_2.HPO_4$), are used as the starting precursors. The phosphate solution of particular molarity is slowly added to an appropriate molar solution of calcium nitrate to form milky precipitate. The milky precipitate is then stirred continuously for particular time and allowed to age. The filtered powder is then dried and sintered. The detail synthesis process of HAp is reported in our earlier work **[12].**

Ion exchange treatment

Cobalt nitrate solutions ($Co(NO_3).6H_2O$) of variable molar concentrations are prepared and a known amount of synthesized nano-HAp is added to each solution. These solutions are thoroughly shaken for 5 hours to have saturation equilibrium and are allowed to settle for about 12 hours. After the ion-exchange treatment, the filtered powder is washed with double distilled water and finally dried in air oven at 100 °C for 10 h. Calcium has ionic radius of 0.99Å whereas ionic radius of cobalt is observed to be 0.745Å. Moreover, oxidation state of both these ions is 2. Therefore, it is expected that Co ions may easily replace Ca ions during ion exchange process.

Thick film preparation

A sensor material is prepared in the form of paste by mixing an appropriate amount of functional material (HAp) and the binders such as glass frit, butyl carbitol acetate & ethyl cellulose by maintaining inorganic to organic ratio 70:30. The HAp thick films, with dimensions of 1 x 1 cm^2, are screen printed on the pre-cleaned glass substrates and sintered at temperatures 750 ^oC for 1 hour to have appropriate adhesion. The details of HAp thick film preparation are reported elsewhere **[11-12].** Gas sensing experiment is carried out using these sintered films. For dielectric measurements the films are prepared in the form of MIM type structure (Ag-HAp-Ag).

Characterization

X-ray diffraction profiles are obtained using Bruker AXS Germany (Model D8 Advanced) make X-ray diffractometer having CuKα (λ= 1.5405 Å) as the incident radiation. For XRD pattern, each sample is scanned in the 2θ range of 20– 60°. The surface topography of the pure & Co-HAp thick film is visualized by means of Atomic Force Microscopy using (Nanoscope IIIa model) from digital/Vecco instruments Inc. The surface morphology is visualized by means of Scanning Electron Microscope (Vega TESCAN). The FTIR spectrum is obtained using Shimadzu make FTIR spectrometer in the range 400-4000 cm^{-1}.

Gas sensing characteristics

The studies on CO_2 gas response of pure and cobalt doped HAp films are carried out using a homebuilt gas sensor chamber as described in our earlier work **[11-12].** CO_2 gas of 1000 ppm in air is used as a standard gas. The electrical resistances in air atmosphere (R_a) and in the presence of particular CO_2 gas concentration (R_g) are determined. The gas response S (%) is calculated as per the formula-

$$\text{Gas response S (\%)} = [\ Rg - Ra\ ] / Ra * 100 \quad (1)$$

Dielectric measurements

The dielectric measurements of pure and ion exchanged Co-HAp films, are also carried out wherein the capacitance (Cp) and dielectric loss (δ) are recorded using Quad Tech make 7600 precision LCR meter. The measurements are carried out at room temperature in the frequency range 10 Hz to 1 MHz. The dielectric constant (K) is determined by using the following formula **[10].**

$$K = Cp \times t / \varepsilon_0 \times A \qquad (2)$$

where, Cp is the capacitance of the sample, t is the thickness of the sample, ε_0 is the permittivity of the vacuum (8.85×10^{-12} F/m), and A is the area of cross-section of the film samples.

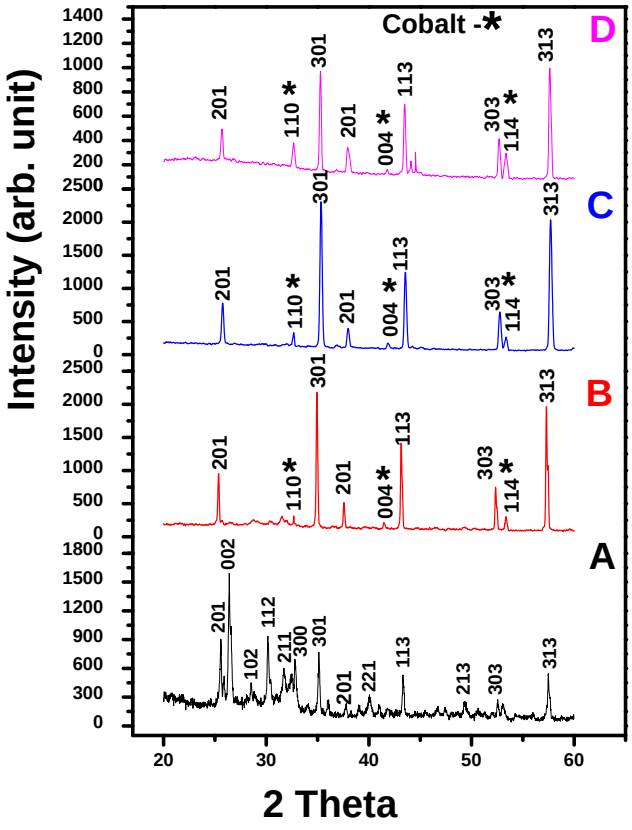

Fig. 1 a-d. XRD patterns of pure and doped HAp thick films; (A) pure HAp film,(B) 0.008 M Co-HAp film (C) 0.01 M Co-HAp film (D) 0.05 M Co-HAp film.

Results and discussion

X-ray analysis

As shown in **Fig. 1(a-d)**, all the diffraction peaks of pure and doped film samples can be readily indexed to hexagonal HAp phase (JCPDS card no. 09-432) and the ion exchanged films show impurity peaks at 2θ values of 32.68, 41.09 and 53.36 due to cobalt ions suggesting that cobalt ions are included in HAp matrix (JCPDS card no.01-1278). In addition, the cobalt inclusion also improves the crystallinity of the products as revealed by the increased peak intensity upto 0.01M cobalt concentration and further increase in cobalt ion concentration (0.5M) results in decrease in intensity (**Fig. 1 (D)**). The crystallite size, calculated by using Debye Scherer's equation **[10],** is found to be around 37 nm for pure HAp thick film and that calculated for cobalt doped HAp with molar concentrations 0.008, 0.01, 0.05 M are found to be 56 nm, 30 nm, 43 nm, respectively.

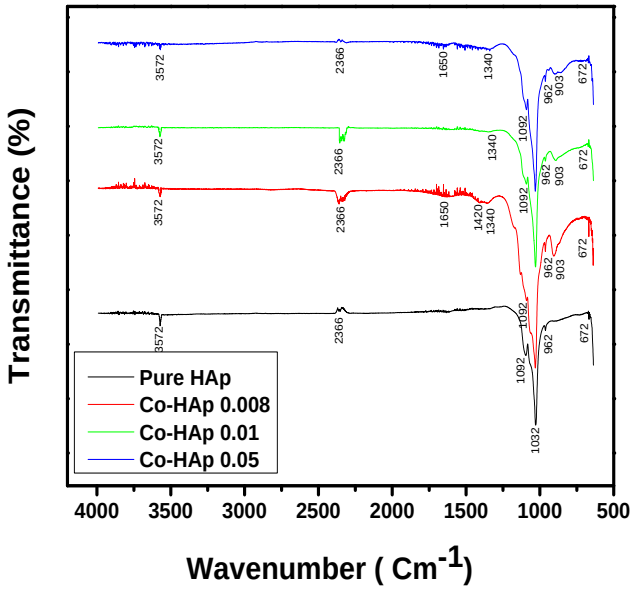

Fig. 2 a-d. FTIR spectra of pure HAp and Co-HAp thick films showing the presence of functional groups (A) pure HAp film, (B) 0.008 M Co-HAp film (C) 0.01 M Co-HAp film (D) 0.05 M Co-HAp film.

FTIR analysis

Representative FTIR spectra, recorded at room temperature in the wave number range 4000 and 400 cm^{-1}, are shown in **Fig. 2(a-d).** The spectra show the presence of characteristic bands of hydroxyl and phosphate species. The absorption band appearing at 3572 cm^{-1} corresponds to the stretching vibration of the hydroxyl group **[10].** The absorption bands at 1032 and 1092 cm^{-1} are due to ν_3 stretching of the phosphate groups (PO_4^{3-}). The bands present at 903–962 cm^{-1} are attributed to ν_1 stretching mode of PO_4^{3-} **[36].** The band at about 1430 cm^{-1} is assigned to CO_3^{2-} ions. In addition to these peaks, the partial replacement of Ca^{2+} by Co^{2+} results in the appearance of new phosphate peak at 903 cm^{-1}. The intensity of this newly developed peak goes on decreasing with increase in cobalt concentration. For higher cobalt concentration (0.05 M), this phosphate peak is converted into doublet form.

SEM analysis

The surface morphology of pure and Co-HAp thick film, visualized by means of Scanning Electron Microscopy (SEM), is presented in **Fig. 3(a-d). Fig. 3a** represents SEM image of pure HAp film surface, wherein number of separate grains are observed. The SEM micrograph of Co-HAp film with a concentration of 0.01 M shows the presence of small particles of variable sizes and shapes

along with micropores. This indicates the suitability of the surface for gas sensing. However, Co-HAp films with concentrations like 0.008M & 0.05M show the formation of cluster type structure.

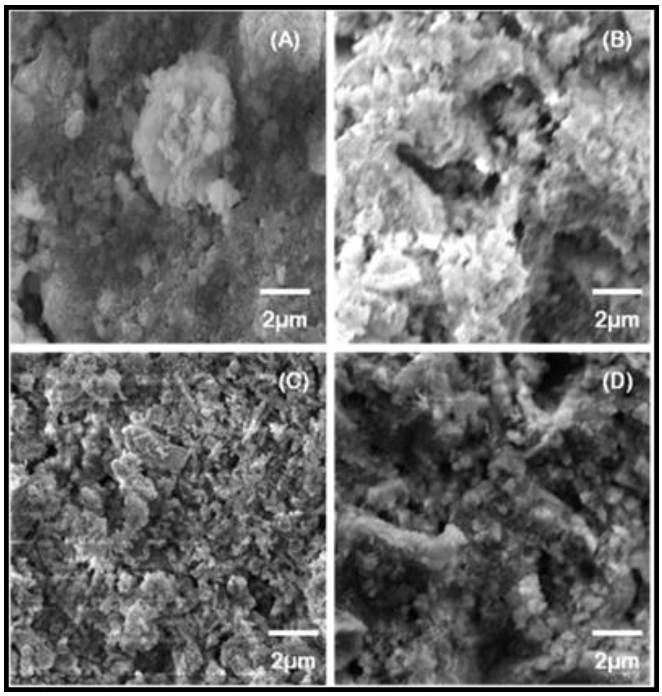

Fig. 3 a-d. SEM images of Pure HAp and Cobalt doped HAp thick films with variable molar concentration A) pure HAp B) 0.008, C) 0.01, and D) 0.05 M.

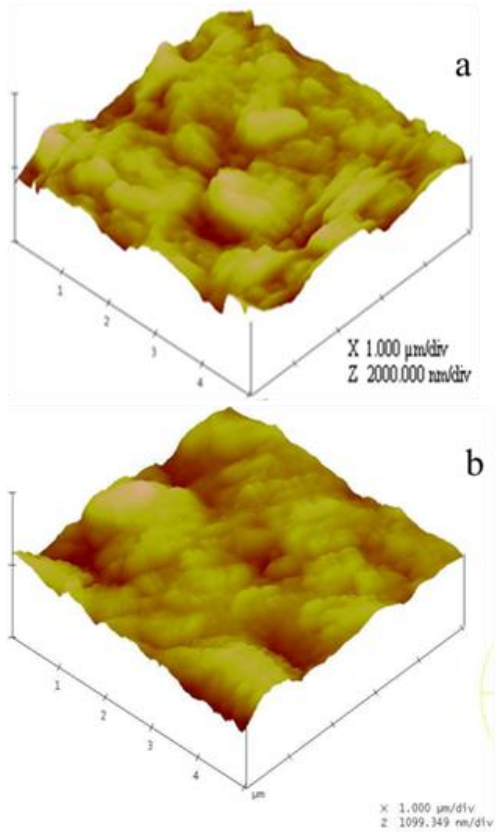

Fig. 4a-b. AFM images of pure HAp and cobalt doped HAp (0.01M) thick films.

AFM analysis

The surface topography of pure and Co-HAp (0.01 M) thick films, observed by means of Atomic Force Microscopy (AFM), is depicted in **Fig. 4 (a-d).** The surface of pure HAp film shows the appearance of variable size grains as presented in **Fig. 4(a).** However, smaller grains are observed on the surface of cobalt doped HAp film **(Fig. 4b)**. These results are coherent with SEM analysis. The root mean square values of surface roughness, evaluated from the AFM, are found to be 78 nm, 127 nm, for pure and Co-HAp (0.01M) respectively.

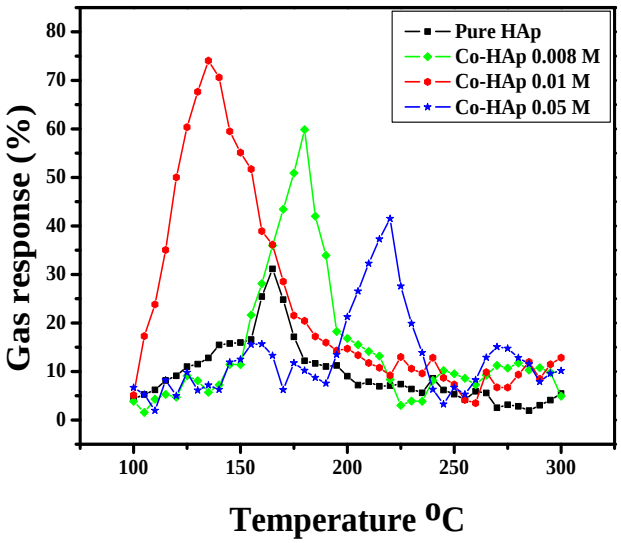

Fig. 5. Variation in gas response as a function of temperature for pure and Co-HAp thick films in response to 1000 ppm CO_2 gas: Pure HAp, Co-HAp (0.008M), Co-HAp (0.01M), Co-HAp (0.05M).

Gas sensing performance of Cobalt doped HAp thick film

Fig. 5 shows change in gas response (%) with temperature for pure and Co-HAp film sensors for 1000 ppm of CO_2 gas. The gas response initially remains very low at lower temperatures and increases with increase in temperature. With further increase in temperature, it goes on decreasing. The gas response shows a maximum which corresponds to operating temperature of the sensor film. For pure HAp thick film, the gas response is found to be 31 at an operating temperature 165°C. Doped films exhibit higher response to CO_2 gas than that of pure films and this reveals that these films are more sensitive to CO_2 gas. In case of doped films, it is observed that gas response and operating temperature depend on cobalt concentration in HAp matrix. The CO_2 gas sensitivity is observed to be small (60) when the cobalt concentration is small (0.008M) with slight shift in operating temperature to the higher side (180). For higher cobalt concentration (0.05M), the sensitivity noticeably again gets suppressed to magnitude of 42 but operation temperature observed to be still higher (220). However, only when the concentration is at a suitable level (0.01M), the sensor gives rise to a large sensitivity value (75) and can be operated at lower operating temperature (135). It can be concluded that inclusion of cobalt ions in

HAp leads to increase in gas response and shift in operating temperature. Thus, the partial substitution of Co^{2+} ions in HAp matrix is found to be beneficial for its use as a CO_2 gas sensor at relatively lower operating temperature.

It may be due to the fact that at a lower concentration of an additive, the newly generated sites are less in number for the gas adsorption. Therefore, all the gas molecules do not get adsorbed. In heavily doped material, the additives may flow over the functional material and may lead to decrease in gas response. However, addition of specific amount of metal additive observed to produce new gas adsorption sites on sensor surface resulting in maximum gas response **[37].** In our study, the specific concentration of cobalt in hydroxyapatite, which results in maximum enhancement for CO_2 gas response, is 0.01M.

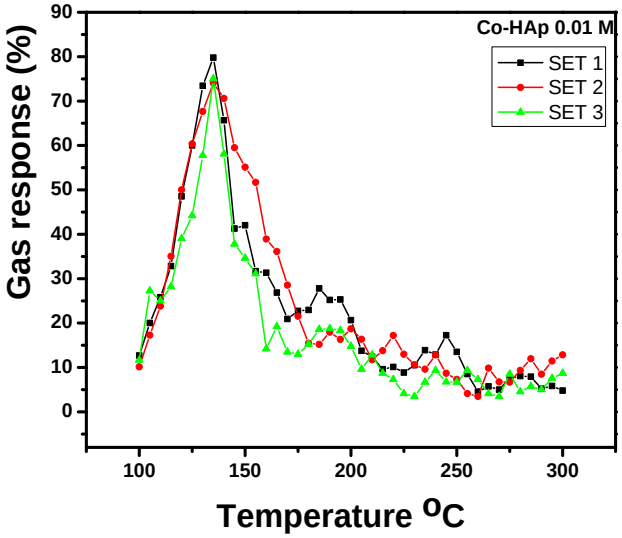

Fig. 6. Gas response as a function of temperature showing repeatability of cobalt doped HAp (0.01M) films for 1000 ppm CO_2 gas.

Fig. 6 shows the repeatability of Co-HAp (0.01 M) thick film. The film is scanned for three times to confirm the operating temperature and gas response for CO_2 gas. The graph reveals the stable performance of Co-HAp (0.01M) film with an operating temperature of 135°C with constant gas response of about 75. The variation in gas response as a function of time is presented in **Fig. 7.** It can be observed that gas response increases with time due to its exposure to CO_2 gas and decreases to its initial value upon air exposure. It is observed that the time required for a pure HAp film to reach to its saturation response limit upon gas exposure, response time, is observed to be 20 sec and that for doped film with a specific concentration is found be 35 sec. The doped films with other concentrations (0.008 and 0.05) take higher time to give response to the same gas. Recovery time is defined as the time needed to reach to original gas response value when exposed to air atmosphere. The recovery times are observed to be 15 sec, 55 sec, 45 sec, 60 sec for a pure film and cobalt doped HAp films respectively. However, the response and recovery times for pure HAp thick film are observed to be smaller than that for Co-HAp films. The cobalt doped film shows high reproducibility upon repeated exposure and removal of CO_2 gas, depicting long-term stability and stable response of the Co-HAp sensor.

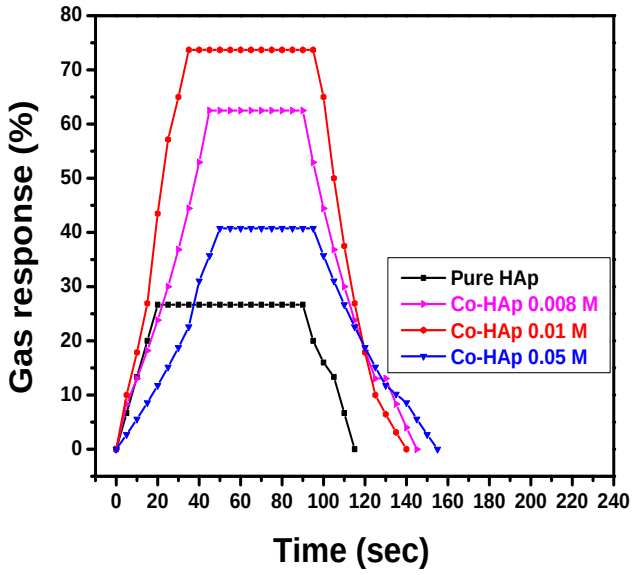

Fig. 7. Response and Recovery times for pure HAp and Co- HAp thick films for 1000 ppm CO_2 gas concentration. [Inset] continues cycles of response and recovery time of Co-HAp (0.01 M) thick film.

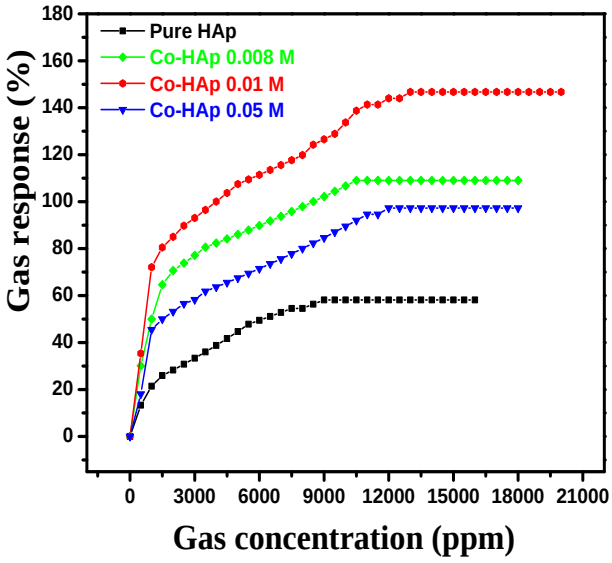

Fig. 8. Variation of Gas response as a function of CO_2 gas concentration for pure and Co-HAp films with various molar concentration 0.008, 0.01, and 0.05 M.

Fig. 8 shows the gas response as a function of CO_2 gas concentration from 500 to 25,000 ppm. Pure HAp film is able to give response up to 9000 ppm CO_2 gas and show saturation thereafter. The Co-HAp film with 0.01 M concentration can sense a CO_2 gas of 13,000 ppm concentration and it gets completely saturated for higher gas load. However, gas upload capacities of Co-HAp films with other concentration (0.008 & 0.05M) are observed to be lower than that of Co-HAp (0.01M). Partial replacement of calcium ions by cobalt ions results in increase in gas upload capacity of pure HAp.

Table 1. Details about structural, sensing and dielectric parameters for pure and Co-HAp thick films with variable concentration (CO_2 gas sensing parameters)

Samples	Size (nm)	Opera. Temp. (^oC)	Gas resp. (%)	Res. Time (Sec)	Res. Time (Sec)	Uptake Cap. (ppm)	DC (K) (100Hz)	Loss (δ) (100Hz)
Pure HAp	37	165	31	20	15	9,000	11	0.21
Co-HAp (0.008M)	56	180	60	45	55	10,500	15	0.18
Co-HAp (0.01M)	30	135	75	35	45	13,000	17	0.16
Co-HAp (0.05M)	43	220	42	50	60	12,000	21	0.15

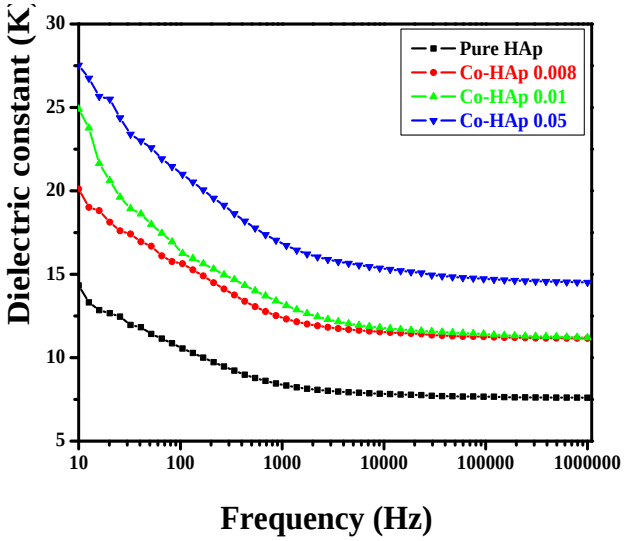

Fig. 9. Variation of dielectric constant as a function of frequency for pure and Co-HAp with molar concentration 0.008, 0.01, and 0.05 M.

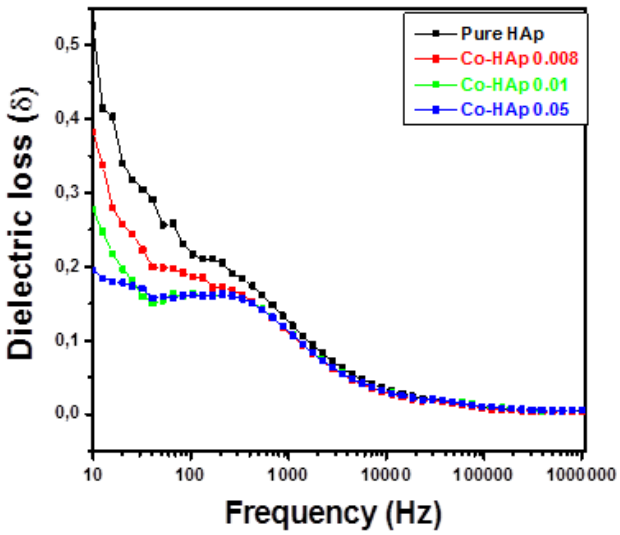

Fig. 10. Variation of dielectric loss as a function of frequency for pure and Co-HAp with molar concentration 0.008, 0.01, and 0.05 M.

The hydroxyapatite possesses porous structure and the hydroxyapatite surface contains variety of ionic species like Ca^{2+}, PO_4^{3-} & OH^-. It is observed that $(OH)^-$ ions interact very effectively with the gas species (CO_2) that adsorbed on the surface **[38-39]** to form CO_3^{2-} molecules. The formation of carbonate group on the surface is an indication that the CO_2 gas has been sensed by material [6,7]. The reaction between neighboring two OH- ions is as follows **[51,52].**

$$OH^- + OH^- \longrightarrow O^{2-} + HOH \quad (3)$$

$$CO_2 + O^{2-} \longrightarrow CO_3^{2-} \quad (4)$$

Moreover, HAp matrix, being nano-sized, provides large surface-to-volume ratio and work as the host with favorable adsorption sites for CO_2 gas **[1-4].** The presence of specific cobalt concentration plays a role of catalytic activator by increasing the gas adsorption sites. Therefore, larger number of CO_2 gas molecules can adsorbed in comparison with the pure HAp, resulting in higher sensitivity for CO_2 gas and that too at comparatively lower operating temperature.

Dielectric study

Fig. 9 manifests the typical dielectric constant (K) profiles for pure and Co-HAp thick films as a function of frequency of applied ac field. The dielectric constant is observed to be the function of frequency of applied ac field and cobalt concentration. It is revealed that dielectric constant decreases with increase in frequency and decrease in cobalt concentration. The values of dielectric constant are quite compatible with the values reported in the literature for HAp **[40-43]**. The dielectric loss also exhibits similar behavior with increasing frequency and is shown in **Fig. 10.** Pure HAp film shows maximum loss. The loss goes on decreasing with increase in cobalt concentration in HAp matrix. The values of dielectric constant and dielectric loss are presented in Table I. Typical complex impedance plot for pure and Co-HAp thick films are shown in **Fig 11 a-d.** The Cole-Cole plot for pure HAp film shows the straight line behavior. This indicates that dielectric relaxation is not possible in these frequency ranges. As the concentration of cobalt increases, the Z" values are found to be decreasing. The Co-HAp film with highest concentration of 0.05 M

shows semicircular behavior which reveals that for this concentration relaxation is possible.

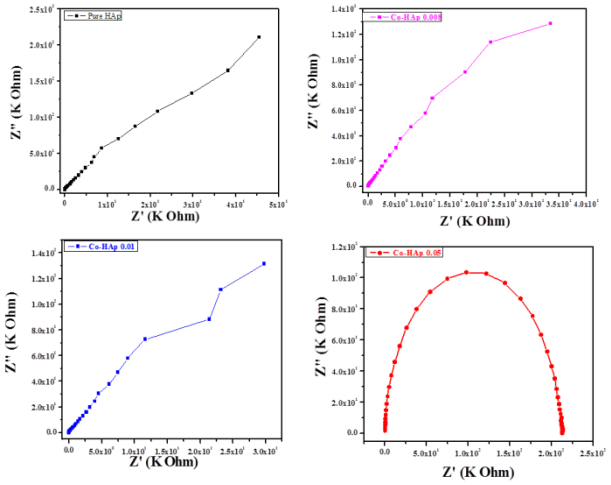

Fig. 11. Complex impedance plot for pure HAp and Co-HAp with molar concentration 0.008, 0.01, and 0.05 M.

The HAp structure contains several ionic species such as Ca^{2+}, $(PO_4)^{3-}$ and especially $(OH)^-$ which are present along c-axis in the form of channel. The major dielectric contribution in HAp is due to the dipole moment of hydroxyl ions along with small electronic contribution as HAp bioceramic is ionic in nature **[10,36,38].** Dielectric constant is due to the polarization in the material. From the frequency response of the dielectric constant, it is found that the dielectric constant is higher at low frequencies because the frequency of electric field is equal to that of natural frequency of bound charge (OH^-) which tends to oscillate the molecules. Moreover, at low frequencies ionic and electronic polarization mechanisms are also operative and contribute to dielectric constant. The decrease of polarization in dielectric material with increasing frequency is due to the fact that beyond certain frequency of the electric field, the ionic displacement cannot follow the electric field due to there high mass and low mobility. If the frequency of the alternating field increases, the ionic dipole moment cannot cope up with field and the alteration of their direction lags behind the field. As a result, the dielectric constant of a material decreases as the frequency applied ac filed is increased still further **[44].** Higher dielectric loss at low frequencies is attributed to oscillations of dipoles. At higher frequencies, ionic polarization ceases and hence energy is not spent to rotate dipoles. Therefore, dielectric loss is found to be lower. Higher dielectric constant for higher Co^{2+} concentration reveals that the inclusion of Co^{2+} ions in HAp matrix becomes more insulating compared to pure HAp, which may find application in high-k devices in microwave electronic area.

Conclusion

Partial substitution of Co^{2+} ions in hydroxyapatite matrix is found to alter gas characteristics such gas response, gas uptake capacity and response/recovery times of HAp thick films. Gas characteristics show anomalous behavior with respect to cobalt concentration. A Co-HAp film with 0.01 M concentration shows maximum gas response, highest gas uptake capacity with a lower temperature of 135°C. The Co-HAp films exhibit remarkable enhancement in dielectric constant compared with pure HAp. Increase in cobalt concentration leads to increase in dielectric constant for HAp films.

Acknowledgements

Thanks are due to Dr. Sunit Rane, C-MET, Pune, for providing experimental facility for preparation of glass frit. Thanks to Prof S G Gosavi for providing SEM characterization facilities. This work is carried out under research project (F.No.SR/S2/CMP-74/2006) sanctioned by Department of Science & Technology (DST), New Delhi, India.

Reference

1. Pandi, G.; Ramaiah, S. *Pure Appl. Chem*. **2008**, *80*, 2377. **DOI:** 10.1351/pac200880112377
2. Iijima, S. *Nature.* **1991**, *354*, 56. **DOI:**10.1038/354056a0
3. De Heer, W.A.; Chatelain, A.; Ugarte, D. *J. Phys. Sci.***2009**, *20*, 27. **DOI:**10.1126/science.270.5239.1179
4. Odom, T.W.; Huang, J.L.; Kim, P.; Lieber, C.M. *Nature***1998,** *391*, 62. **DOI:**1998;391:62–4
5. Santos, C.V.; Hernandez, A.L.M.; Fisher, F.T. *Chem. Mater.***2003,** *15*, 4470. **DOI:**2003;15(23):4470–5
6. Zhong, H.; Yuan, R.; Chai, Y.; Li, W.; Zhong, X. *Talanta.***2011**, *85*, 104. **DOI:**10.1016/j.talanta.2011.03.040
7. Heeger, A.J. *J. Phys. Chem. B.***2001**, *105(36)*, 8475. **DOI:** 10.1002/1521-3773(20010716)40
8. Konyushenko, E.N.; Stejskal, J.; Trchova, M.; Hradil, J.; Kovarova, J.; Prokes, J.; Cieslar, M.; Hwang, J.Y.; Chen, K.H.; Sapurina, I. *Polymer*. **2006**, *47(16)*, 5715. **DOI:**10.1016/j.polymer.2006.05.059
9. Peng, C.; Jin, J.; Chen, G.Z. *Electrochim. Acta*. **2007**, *53(2)*, 525. **DOI:**10.1016/j.electacta.2007.07.004
10. Jiang, J.; Kucernak, A. *Electrochim. Acta*. **2002**, *47(15)*, 2381. **DOI:**10.1016/S0013-4686(02)00031-2
11. Zein, S.H.S.; Yeoh, L.C.; Chai, S.P.; Mohamed, A.R.; Mahayuddin, M.E.M. *J. Mat. Proc. Tech.***2007**, *190(1)*, 402. **DOI:**10.1016/j.jmatprotec.2007.03.104
12. McCall, R.P.; Ginder, J.M.; Leng, J.M.; Ye, H.J.; Manohar, S.K.; Masters, J.G. *Phys Rev B*, **1990**, *41*, 5202. **DOI:**10.1103/PhysRevB.41.5202
13. Scherr, E.M.; MacDiarmid, A.G.; Monahar, S.K.; Masters, J.G.; Sun, Y.; Tang, X. *Synth. Met.***1991**, *41(1)*, 735. **DOI:**10.1016/0379-6779(91)91173-8
14. Xia, H.; Wang, Q. *J. Appl. Polym. Sci.*, **2003**, *87(11)*, 1811. **DOI:**10.1002/app.11627
15. Bavastrello, V.; Terencio, T.B.C.; Nicolini, C.; *Polymer* **2011**, *52(1)*, 46. **DOI:**10.1016/j.polymer.2010.10.022
16. Quillard, S.; Louarn, G.; Lefrant, S.; MacDiarmid, A.G. *Phy. Rev. B*, **1994**, *50(17)*, 12496. **DOI:**10.1103/PhysRevB.50.12496
17. Cochet, M.; Maser, W.K.; Benito, A.M.; Callejas, M.A.; Martinez, M.T.; Benoit, J.M.; Schreiber, J.; Chauvet, O. *Chem. Commun.***2001**, *16*, 1450. **DOI:**10.1039/B104009J

